Proceedings of the 29th Annual International
Conference of the IEEE EMBS
Cité Internationale, Lyon, France
August 23-26, 2007.

Robustness of Local Binary Patterns in Brain MR Image Analysis*

Devrim Unay, Ahmet Ekin, Mujdat Cetin, Radu Jasinschi, and Aytul Ercil

***Abstract*—The aging population in developed countries has shifted considerable research attention to diseases related to age. Because age is one of the highest risk factors for neurodegenerative diseases, the need for automated brain image analysis has significantly increased. Magnetic Resonance Imaging (MRI) is a commonly used modality to image brain. MRI provides high tissue contrast; hence, the existing brain image analysis methods have often preferred the intensity information to others, such as texture. Recently, an easy-to-compute texture descriptor, Local Binary Pattern (LBP), has shown promise in various applications outside the medical field. In this paper, after extensive experiments, we show that rotation-invariant LBP is invariant to some common MRI artifacts that makes it possible to use it in various high-level brain MR image analysis applications.**

I. Introduction

Automated and robust brain image analysis has a number of applications ranging from diagnosis to understanding of neurodegenerative diseases. MRI is the preferred modality for imaging the brain as it provides excellent intensity contrast among tissue types. Partly because of this, the literature has mainly concentrated on using MR intensity values in the analysis of brain MR images. The structural information in the form of texture has been computational to extract although texture information can complement MR intensity and remedy some of the inherent intensity-related problems.

Recently, an easy-to-compute, robust local texture descriptor, Local Binary Pattern (LBP) [1], has been shown to be promising in the computer vision field, including industrial inspection [2], motion analysis [3], and face recognition [4]. However, in medical image processing, its application has been mainly limited to endoscopic [5] and ultrasound images [6]. In this paper, we show that LBP can solve some of the inherent intensity-related MR problems, is robust to some geometric deformations, and has potential for further applications.

For instance, in MRI, image intensity smoothly varies across an image [7]-[9]. This intensity inhomogeneity, or so-called bias field, can significantly degrade the performance of automatic segmentation techniques. Because the bias field is locally smooth, we argue that it should not change the local structure.

Furthermore, in MR acquisition inter- and intra-patient misalignment of the images is a known problem, which can be severe in patients with neurodegenerative diseases, (e.g. those with Parkinson's). This misalignment problem may limit the application of automated tools on MR images of such data. In this case, rotation invariant descriptors may prevent some of those limitations.

In this paper, after rigorously testing LBP and its variants on a large set of real MR brain data affected by various forms of bias fields, we show that LBP is robust to bias field and rotation. This paper is organized as follows: Section II introduces a theoretical framework for LBP. Section III describes the applications of LBP to MR brain image analysis. Section IV explains the experimental data and subsequently details the two experiments performed in this study. Finally, Section V concludes this paper.

II. Local Binary Patterns

LBP is a grayscale invariant local texture operator with powerful discrimination and low computational complexity. An LBP operator thresholds a neighborhood by the gray value of its center (g_c) and represents the result as a binary code that describes the local texture pattern. The operator ($LBP_{P,R}$) is derived based on a symmetric neighbor set of P members $g_p(p=0,\cdots,P-1)$ within a circular radius of R.

$$LBP_{P,R}=\sum_{p=0}^{P-1}s(g_p-g_c)2^p \tag{1}$$

where

$$s(x)=\begin{cases}1, x\geq 0\\ 0, x<0.\end{cases} \tag{2}$$

Fig. 1 illustrates the computation of $LBP_{8,1}$ for a single pixel in a rectangular 3x3 neighborhood.

In the general definition, LBP is defined in a circular

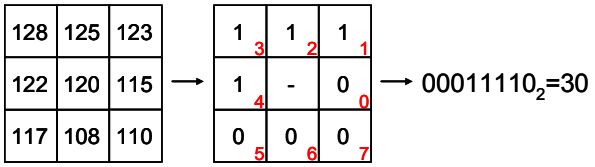

Fig. 1. Example of computing $LBP_{8,1}$: a pixel neighborhood (left), its thresholded version (middle), and the corresponding binary LBP pattern with the computed LBP code (right).

* This work has been conducted as part of the IRonDB project MTKI-CT-2006-042717 under the FP6 Marie Curie Transfer of Knowledge Programme. D. Unay is fully supported by MTKI-CT-2006-042717.

D. Unay, A. Ekin and R. Jasinschi are with the Video Processing and Analysis Group, Philips Research Europe, 5656 AE Eindhoven, The Netherlands (devrim.unay@philips.com, ahmet.ekin@philips.com, radu.jasinschi@philips.com)

M. Cetin and A. Ercil are with the Faculty of Engineering and Natural Sciences, Sabanci University, 34956, Tuzla-Istanbul, Turkey (mcetin@sabanciuniv.edu, aytulercil@sabanciuniv.edu)

Authorized licensed use limited to: ULAKBIM UASL - SABANCI UNIVERSITY. Downloaded on June 16, 2009 at 02:31 from IEEE Xplore. Restrictions apply.

symmetric neighborhood which requires interpolation of intensity values for exact computation. In order to keep computation simple, in this study we decided to use the three rectangular neighborhoods as shown in Fig. 2.

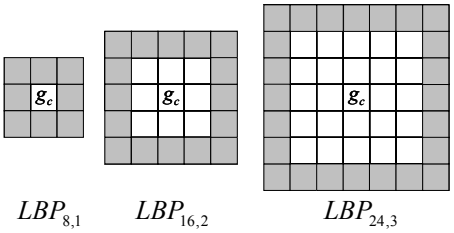

Fig. 2. The rectangular neighborhoods of LBP used in this study. Gray-shaded rectangles refer to the pixels belonging to the corresponding neighborhood.

A. Rotation Invariant Patterns

The $LBP_{P,R}$ operator can produce 2^P different output values from the *P* neighbor pixels. As g_0 is always assigned to be the gray value of neighbor to the right of g_c, rotation will result in a different $LBP_{P,R}$ value for the same binary pattern. One way to eliminate the effect of rotation is to perform a bitwise shift operation on the binary pattern P-1 times and assign the LBP value that is the smallest, which is now referred to as $LBP^{ri}_{P,R}$ (Fig. 3).

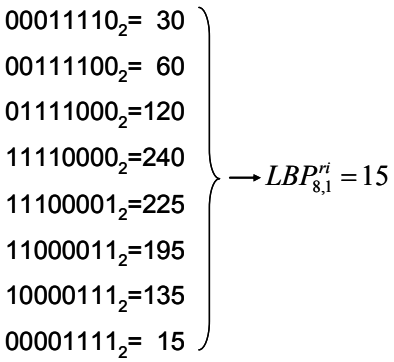

Fig. 3. Example of computing rotation invariant LBP.

B. "Uniform" Patterns

A binary pattern is called "uniform" if it contains at most 2 spatial transitions (bitwise 0/1 changes) [1]. Based on this uniformity concept, a new LBP value ($LBP^{riu2}_{P,R}$) can be computed by summing the bit values of a rotation invariant binary pattern if it is uniform, or a miscellaneous label P+1 can be assigned if it is nonuniform (Fig. 4).

$LBP^{ri}_{8,1}$	spatial transitions	$LBP^{riu2}_{8,1}$
00000000_2	0	0
11111111_2	0	8
00000001_2	2	1
00000011_2	2	2
00001011_2	4	9

Fig. 4. Example of computing rotation invariant and uniform LBP.

In this study, robustness of simple ($LBP_{P,R}$), rotation invariant ($LBP^{ri}_{P,R}$), and rotation invariant and uniform ($LBP^{riu2}_{P,R}$) LBP features at three different rectangular neighborhoods (Fig. 2) are tested relative to bias field and rotation.

III. Applications of LBP to MR Brain Image Analysis

In MRI patient is subjected to different magnetic fields at specific orientations. The protons (hydrogen atoms) in the patient's body respond to these fields by differential decay and recovery signals, which are acquired by the MR machine and then converted to high contrast images. Due to factors like poor radio-frequency gradient uniformity, static field inhomogeneity, radio-frequency penetration, gradient-driven eddy currents, and patient anatomy and position, pixel intensities in MR images smoothly vary. This variation, known as intensity inhomogeneity/nonuniformity or bias field, has little impact on visual diagnosis, but its impact on the performance of automatic segmentation methods can be catastrophic due to increased overlaps between intensities of different tissues.

Furthermore, acquisition times of MRI are generally in the order of 10-20 minutes, during which patients (especially those with Parkinson's disease) tend to move that results in spatially misaligned images. A common solution for this problem is registration, which may not be favored in some applications due to its computational expense and complexity. Hence, textural descriptors for MR images that are consistent in varying intensities as well as geometric transformations like rotation will be very valuable.

IV. Results

A. Experimental Data

The database used in this study consists of dual (T2 and Proton Density) MR scans from 549 subjects, which are acquired on a Philips Intera 1.5T whole body scanner at Leiden University Medical Center. We used dual-spin echo weighted images (TR/TE1/TE2: 3000/27/120 ms, FLIP: 90) with 220mm FOV, 3mm slice thickness, no slice gap and 256x256 matrix.

In order to test robustness of LBP with respect to intensity variations, three simulated bias fields from the BrainWeb MR simulator [10] are used (Fig. 5). These bias fields provide smooth variations of intensity across the image. Furthermore, we applied linear transformation to obtain a new bias field of each with 10%, 20%, 30% and 40%

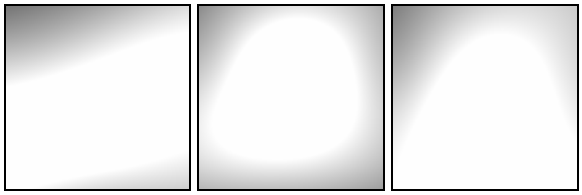

Fig. 5. Examples of simulated bias fields used in this study, where intensity variations are exaggerated for visual purposes.

Authorized licensed use limited to: ULAKBIM UASL - SABANCI UNIVERSITY. Downloaded on June 16, 2009 at 02:31 from IEEE Xplore. Restrictions apply.

intensity variations. Based on the conventional assumption that the bias field in MR images is multiplicative [7]-[9], we degraded the original images by multiplying them with the resulting bias fields.

B. Evaluation Method

The degree of dissimilarity between the LBP values of the original and the degraded (by the bias field and rotation) images is computed on the corresponding normalized LBP histograms using the Bhattacharyya distance (3) and the histogram intersection (4):

$$d_B = 1 - \sum_{i=0}^{L-1} \sqrt{p(i) \cdot q(i)} \tag{3}$$

$$d_I = 1 - \sum_{i=0}^{L-1} \min[p(i), q(i)] \tag{4}$$

where p and q are the two histograms with L-bins. The dissimilarity scores for both measures fall in the range of [0,1], where 0 means that the two images are perfectly similar. Please note that as we observed similar results with both measures for all the tests, the following sections provide the results based on only Bhattacharyya measure.

C. Robustness to Bias Field

We first tested the consistency of LBP relative to the bias field, where several LBP operators are applied on the original images as well as on those degraded by the bias fields. Table I displays dissimilarity scores of this test for all the bias fields and several LBP features, while Fig.6 shows the result of $LBP_{8,1}$. We observe a steady increase in dissimilarity values with the bias field strength. Bias field B provides the highest dissimilarity score for all strengths, because it has larger spatial variation. All the dissimilarity values are below 0.04%, which shows that the LBP features are robust to the bias fields.

TABLE I
EFFECT OF BIAS FIELD ON VARIOUS LBP FEATURES

	$LBP_{8,1}$	$LBP^{ri}_{8,1}$	$LBP^{riu2}_{8,1}$	$LBP_{16,2}$	$LBP^{ri}_{16,2}$	$LBP^{riu2}_{16,2}$	$LBP_{24,3}$	$LBP^{ri}_{24,3}$	$LBP^{riu2}_{24,3}$
A-10	0.25	0.12	0.00	0.59	0.38	0.01	0.64	0.54	0.01
A-20	0.55	0.26	0.01	1.22	0.79	0.01	1.30	1.10	0.02
A-30	0.85	0.40	0.02	1.91	1.17	0.02	1.93	1.68	0.03
A-40	1.17	0.55	0.03	2.48	1.57	0.03	2.54	2.18	0.05
B-10	0.37	0.17	0.01	0.84	0.52	0.01	0.94	0.74	0.01
B-20	0.71	0.33	0.01	1.61	1.02	0.02	1.81	1.50	0.03
B-30	1.03	0.48	0.02	2.38	1.50	0.03	2.62	2.14	0.04
B-40	1.39	0.65	0.03	3.14	1.95	0.04	3.38	2.72	0.05
C-10	0.20	0.09	0.00	0.49	0.32	0.01	0.58	0.52	0.01
C-20	0.46	0.21	0.01	1.09	0.68	0.01	1.21	1.05	0.02
C-30	0.73	0.34	0.02	1.63	1.03	0.02	1.83	1.58	0.03
C-40	1.02	0.47	0.03	2.17	1.38	0.03	2.41	2.05	0.04

Values in the table are the dissimilarity scores (10^{-4}).

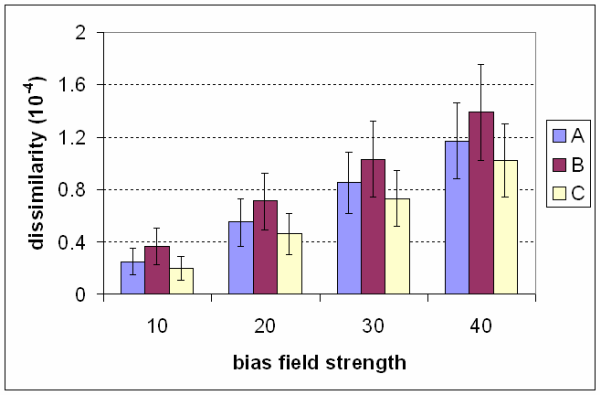

Fig. 6. Robustness of $LBP_{8,1}$ relative to varying bias field strength.

D. Robustness to Rotation

In order to test the robustness of LBP features relative to rotation, we have rotated the original images by 15°, 30°, 45°, and 60° at clockwise and counterclockwise directions using three different interpolation methods: nearest neighbor, bilinear, and bicubic (presented from the simplest to the most complex, respectively). Fig. 7 displays examples of some of the rotated images.

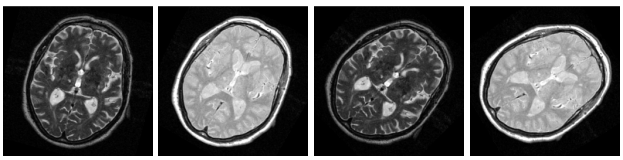

Fig. 7. Examples of T2 (1st and 3rd from the left) and Proton Density (2nd and 4th from the left) images rotated by 15°, 30°, 45° and 60°, respectively using bicubic interpolation.

Table II displays the average dissimilarity scores between the original images and their rotated versions for all the LBP features when the rotation is performed at various angles in both clockwise and counterclockwise directions using three interpolation methods. We generally observe that dissimilarity values decrease when 1) the complexity of the interpolation method increases, 2) the rotation invariancy and the uniformity is introduced to LBP, and 3) the radius of the LBP operator is increased. The former observation is coherent with the fact that the complexity of the interpolation method is directly related to the quality of the resulting rotated image. The second observation is understandable when we consider that the rotation invariant and "uniform" LBP patterns correspond to the primitive microfeatures in the image [1]. Finally, the third observation is meaningful in the sense that as the neighborhood gets bigger, the effect of degradation caused by rotation gets weaker due to the

TABLE II
EFFECT OF ROTATION ON VARIOUS LBP FEATURES

		$LBP_{8,1}$	$LBP^{ri}_{8,1}$	$LBP^{riu2}_{8,1}$	$LBP_{16,2}$	$LBP^{ri}_{16,2}$	$LBP^{riu2}_{16,2}$	$LBP_{24,3}$	$LBP^{ri}_{24,3}$	$LBP^{riu2}_{24,3}$
-60	nearest	4.00	3.05	0.96	0.40	0.30	0.02	0.23	0.20	0.01
-45		4.05	2.98	0.41	0.39	0.39	0.04	0.23	0.22	0.02
-30		3.65	2.83	0.80	0.33	0.27	0.02	0.23	0.21	0.01
-15		1.26	0.99	0.32	0.26	0.23	0.03	0.20	0.15	0.01
15		1.29	1.02	0.41	0.25	0.21	0.02	0.18	0.13	0.01
30		3.66	2.84	1.12	0.33	0.27	0.01	0.20	0.20	0.01
45		4.03	2.95	0.56	0.37	0.37	0.03	0.23	0.22	0.02
60		3.98	2.94	0.94	0.34	0.27	0.02	0.21	0.21	0.01
-60	bilinear	1.27	0.73	0.33	0.32	0.23	0.07	0.18	0.13	0.03
-45		1.12	0.67	0.30	0.30	0.23	0.08	0.19	0.13	0.03
-30		0.86	0.56	0.25	0.29	0.22	0.07	0.18	0.14	0.03
-15		0.73	0.55	0.22	0.25	0.21	0.06	0.17	0.14	0.03
15		0.72	0.54	0.17	0.22	0.23	0.05	0.17	0.12	0.03
30		0.85	0.57	0.15	0.25	0.20	0.05	0.19	0.12	0.02
45		1.09	0.69	0.15	0.28	0.20	0.05	0.17	0.13	0.02
60		1.27	0.73	0.14	0.30	0.21	0.05	0.19	0.12	0.02
-60	bicubic	0.97	0.44	0.12	0.29	0.15	0.02	0.19	0.10	0.01
-45		0.82	0.39	0.10	0.29	0.15	0.02	0.19	0.12	0.01
-30		0.59	0.28	0.07	0.26	0.14	0.01	0.19	0.11	0.01
-15		0.37	0.21	0.05	0.23	0.14	0.01	0.19	0.10	0.01
15		0.38	0.21	0.03	0.21	0.15	0.01	0.17	0.10	0.01
30		0.54	0.26	0.02	0.23	0.13	0.01	0.19	0.10	0.01
45		0.80	0.41	0.03	0.26	0.13	0.01	0.18	0.11	0.01
60		0.99	0.44	0.03	0.27	0.13	0.01	0.18	0.10	0.01

Values in the table are the dissimilarity scores (10^{-2}).

Authorized licensed use limited to: ULAKBIM UASL - SABANCI UNIVERSITY. Downloaded on June 16, 2009 at 02:31 from IEEE Xplore. Restrictions apply.

increased radius as well as higher number of neighbors present.

Fig. 8 and 9 display the effect of the interpolation method and the LBP feature type relative to rotation, respectively. These two figures visually support the observations we made previously: dissimilarity increases with the rotation angle, the complexity of the interpolation method has inverse relation with the dissimilarity, and rotation invariant and uniform LBP features ($LBP_{8,1}^{riu2}$) are the most robust to rotation, while simple LBP features ($LBP_{8,1}$) are the least.

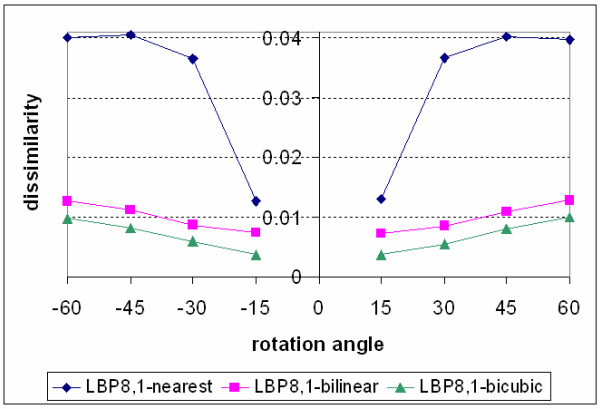

Fig. 8. Robustness of $LBP_{8,1}$ relative to different interpolation methods for rotation.

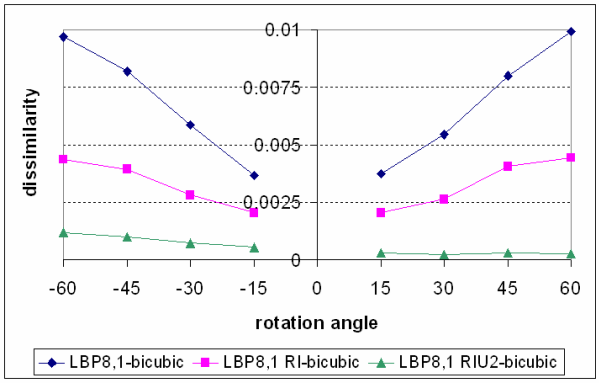

Fig. 9. Robustness of different $LBP_{8,1}$ features relative to rotation by bicubic interpolation.

E. Computational Expense of LBP

We measured the average process time of computing LBP in the range of 60 ($LBP_{8,1}$) - 1100 ($LBP_{24,3}^{rui2}$) ms per slice on an Intel Pentium processor (2.8 GHz) with 1G memory. However, the computation time can be considerably reduced using look-up tables (for rotation invariant and uniform LBP codes: the main bottlenecks of the current implementation that is in C) and optimized software.

V. CONCLUSIONS

MRI provides high tissue contrast, which makes MR the preferred modality to image brain. The existing brain image analysis methods often focus on the intensity information only. LBP is a computationally efficient, gray-scale and rotation invariant texture operator that can provide complementary information for brain image analysis.

In MRI, some common artifacts, like intensity variation across the image and spatial misalignment of images, can pose great difficulties for automatic analysis methods. Hence, LBP that is invariant to gray-scale and rotation may be a robust choice for MR brain image analysis.

Therefore, in this study we tested the robustness of LBP to MR bias field as well as rotation. Results showed that LBP is robust to bias field even at 40% intensity variations. Secondly, original images are rotated by up to 60° in both clockwise and counterclockwise directions using three different interpolation methods. LBP was again found to be robust to rotation.

Results of this study lead to the fact that LBP, which is computationally simple and robust to bias field and rotation, can be a promising texture descriptor in various MR brain image analysis applications, like image normalization, tissue segmentation and abnormality detection.

ACKNOWLEDGMENT

The authors would like to thank the Marie Curie Programme of the European Commission for the support to FP6 IRonDB project MTKI-CT-2006-042717. We also would like to thank Prof. Mark van Buchem and Dr. Jeroen van der Grond from the Department of Radiology, Leiden University Medical Center for the discussions and the data support.

REFERENCES

[1] T. Ojala, M. Peitikäinen, and T. Mäenpää, "Multiresolution gray-scale and rotation invariant texture classification with local binary patterns," *IEEE Trans. Pattern Analysis and. Machine Intelligence,* vol. 24, pp. 971–987, July 2002.

[2] T. Mäenpää, M. Turtinen,and M. Peitikäinen, "Real-time surface inspection by texture", *Real-Time Imaging,* vol. 9, pp. 289–296, 2003.

[3] M. Heikkilä,and M. Peitikäinen, "A texture-based method for modeling the background and detecting moving objects", *IEEE Ttrans. Pattern Analysis and Machine Intelligence,* vol. 28, pp. 657–662, 2006.

[4] T. Ahonen, A. Hadid, and M. Peitikäinen, "Face description with local binary patterns: application to face recognition", ", *IEEE Ttrans. Pattern Analysis and Machine Intelligence,* vol. 28, pp. 2037–2041, 2006.

[5] D. K. Iakovidis, D. E. Maroulis, and S. A. Karkanis, "An intelligent system for automatic detection of gastrointestinal adenomas in video endoscopy", *Computers in Biology and Medicine,* vol. 36, pp. 1084–1103, 2006.

[6] O. Pujol, D. Rotger, P. Radeva, O. Rodriguez, and J. Mauri, "Near real-time plaque segmentation of IVUS", in *Proc. Computers in Cardiology,* Thessaloniki, Greece, September 2003, pp. 69–73.

[7] J. G. Sled, A. P. Zijdenbos, and A. C. Evans, "A nonparametric method for automatic correction of intensity nonuniformity in MRI data", *IEEE Trans. Medical Imaging,* vol. 17, pp.87–97, February 1998.

[8] B. Likar, M. A. Viergever, and F. Pernuš, "Retrospective correction of MR intensity inhomogeneity by information minimization", *IEEE Trans. Medical Imaging,* vol. 20, pp. 1398–1410, December 2001.

[9] U. Vovk, F. Pernuš, and B. Likar, "MRI Intensity inhomogeneity correction by combining intensity and spatial information", *Phys. Med. Biol.,* vol. 49, pp. 4119–4133, 2004.

[10] [Online] http://www.bic.mni.mcgill.ca/brainweb/

Authorized licensed use limited to: ULAKBIM UASL - SABANCI UNIVERSITY. Downloaded on June 16, 2009 at 02:31 from IEEE Xplore. Restrictions apply.